The American Journal of Human Genetics, Volume *101*

Supplemental Data

Mutations in *ARMC9*, which Encodes a Basal Body Protein, Cause Joubert Syndrome in Humans and Ciliopathy Phenotypes in Zebrafish

Julie C. Van De Weghe, Tamara D.S. Rusterholz, Brooke Latour, Megan E. Grout, Kimberly A. Aldinger, Ranad Shaheen, Jennifer C. Dempsey, Sateesh Maddirevula, Yong-Han H. Cheng, Ian G. Phelps, Matthias Gesemann, Himanshu Goel, Ohad S. Birk, Talal Alanzi, Rifaat Rawashdeh, Arif O. Khan, University of Washington Center for Mendelian Genomics, Michael J. Bamshad, Deborah A. Nickerson, Stephan C.F. Neuhauss, William B. Dobyns, Fowzan S. Alkuraya, Ronald Roepman, Ruxandra Bachmann-Gagescu, and Dan Doherty

Supplementary Data

Figure S1: zebrafish *armc9* gene structure and expression

(A) Schematic representation of the zebrafish *armc9* gene (with exonic/intronic structure) and protein below, showing the predicted LisH domain (green, N-terminal) and the armadillo-type-fold (ATF) domain (blue). **(B-K)** *In situ* hybridization on brain cryosections from adult zebrafish (**B-F** transverse sections, **G-K** sagittal sections). **(B)** Note staining along the ventricles marked with the arrows. **(C-E)** Higher magnification views of the boxed areas in **(B). (C)** Ventral zone of periventricular hypothalamus *Hv,* **(D)** periventricular grey zone of optic tectum *PGZ,* **(E)** lateral division of valvula cerebelli *Val* and torus longitudinalis *TL*. **(F)** Absence of staining with the control sense probe. **(G)** Sagittal section through the brain and eye, showing signal in the cerebellum (boxed area **H**), the hypothalamus (boxed area **I**) and the optic tectum (boxed area **J**). *CCe* corpus cerebelli, *LCa* lobus caudalis cerebelli, *H* periventricular hypothalamus, *PGZ* periventricular grey zone of optic tectum, *TL* torus longitudinalis. **(K)** Absence of staining with the control sense probe. Scale bars: 200µm (B,F,G,K), 50µm (C-E), 100 µm (H-J).

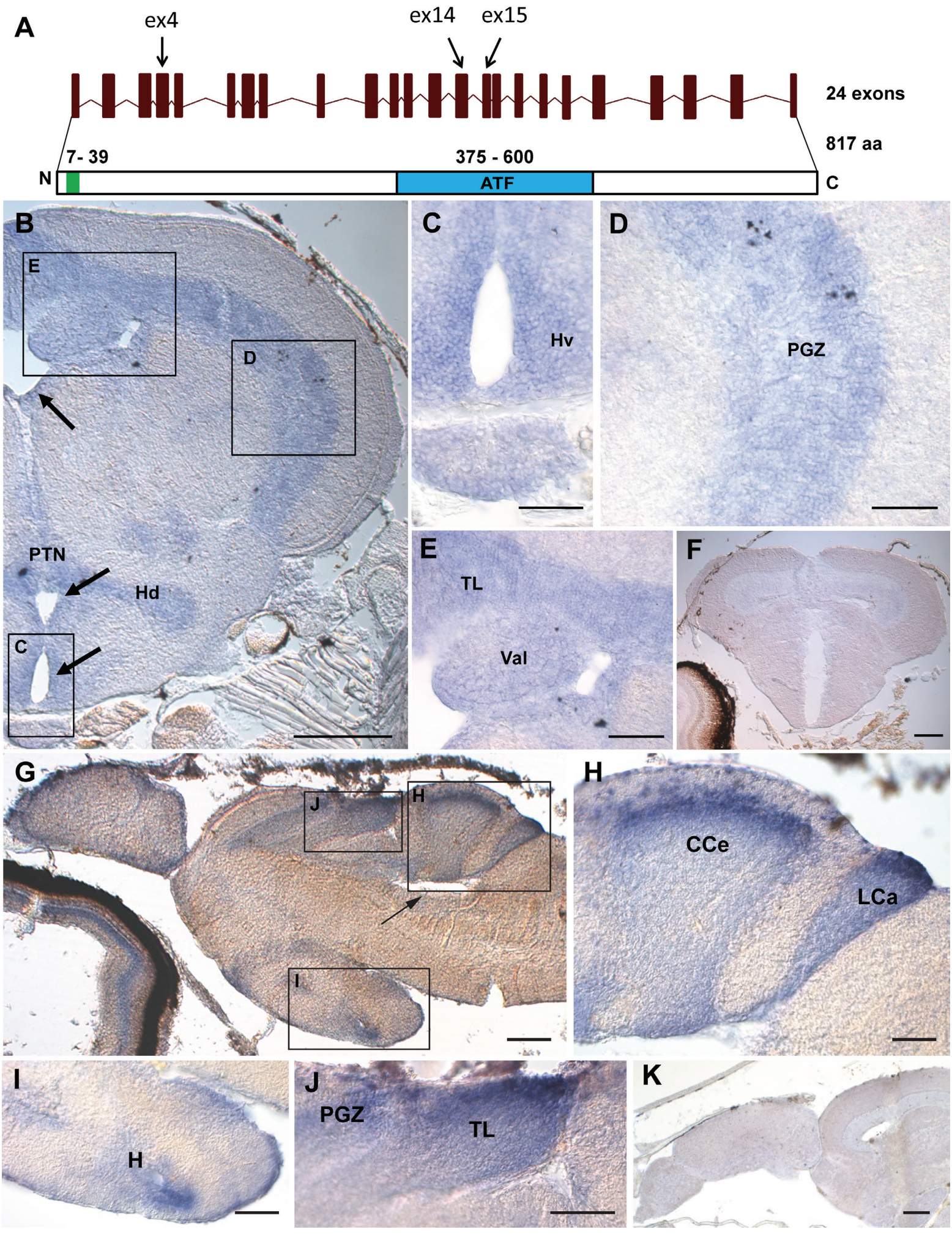
A
ex4
ex14
ex15
24 exons
817 aa
7- 39
375 - 600
N
ATF
C
B
E
D
PTN
Hd
C
C
Hv
D
PGZ
E
TL
Val
F
G
J
H
I
H
CCe
LCa
I
H
J
PGZ
TL
K

Fig S2: CRISPR/Cas9 *armc9* mutants

(A) Representative gel showing PCR amplification around the CRISPR target sites on finclips from adult F0 animals with body curvature. Note the presence of bands in addition to the WT-sized band in the curved fish. The PCR product from animal #2 was cloned and sequenced, revealing that 9 of 9 selected clones had small out-of-frame indels, indicating that this animal had a very high rate of mutations in *armc9* despite a wild-type-sized band on the gel. **(B-C)** Scanning electron microscopy (SEM) overview images of dissected and halved brains from F0 *armc9* animals with body curvature. The arrow points to the ventricular surfaces shown in **(D-E).** **(D-E)** Close up SEM images of the ventricular surface showing bundles of cilia in wild-type animals **(D)**. In contrast, *armc9* F0 mutant animals display a paucity of cilia **(E)**. **(F-I')** Immunohistochemistry on cryosections through whole eyes of wild-type **(F)** and an F0 *armc9* mutant **(G-I')** stained with the zpr1 antibody marking red-green cone cell bodies (red in **F-I**) and DiO highlighting photoreceptor (PR) outer segments (OS) (green in H-I). Note the thinner retinal layers and the coloboma (arrows in **G** and boxed area in **H**). **(I-I'')** represent the boxed area in **(H).** Note the discontinuity of the retinal layers and the presence of a second leaflet of retina folding back, with presence of PRs and OSs in a mirror image on either side of this aberrant second retinal layer (arrows). Scale bars are 100μm in (B-C), 3μm in (D-E), 100μm in (F-H), 50μm in (I'-I'').

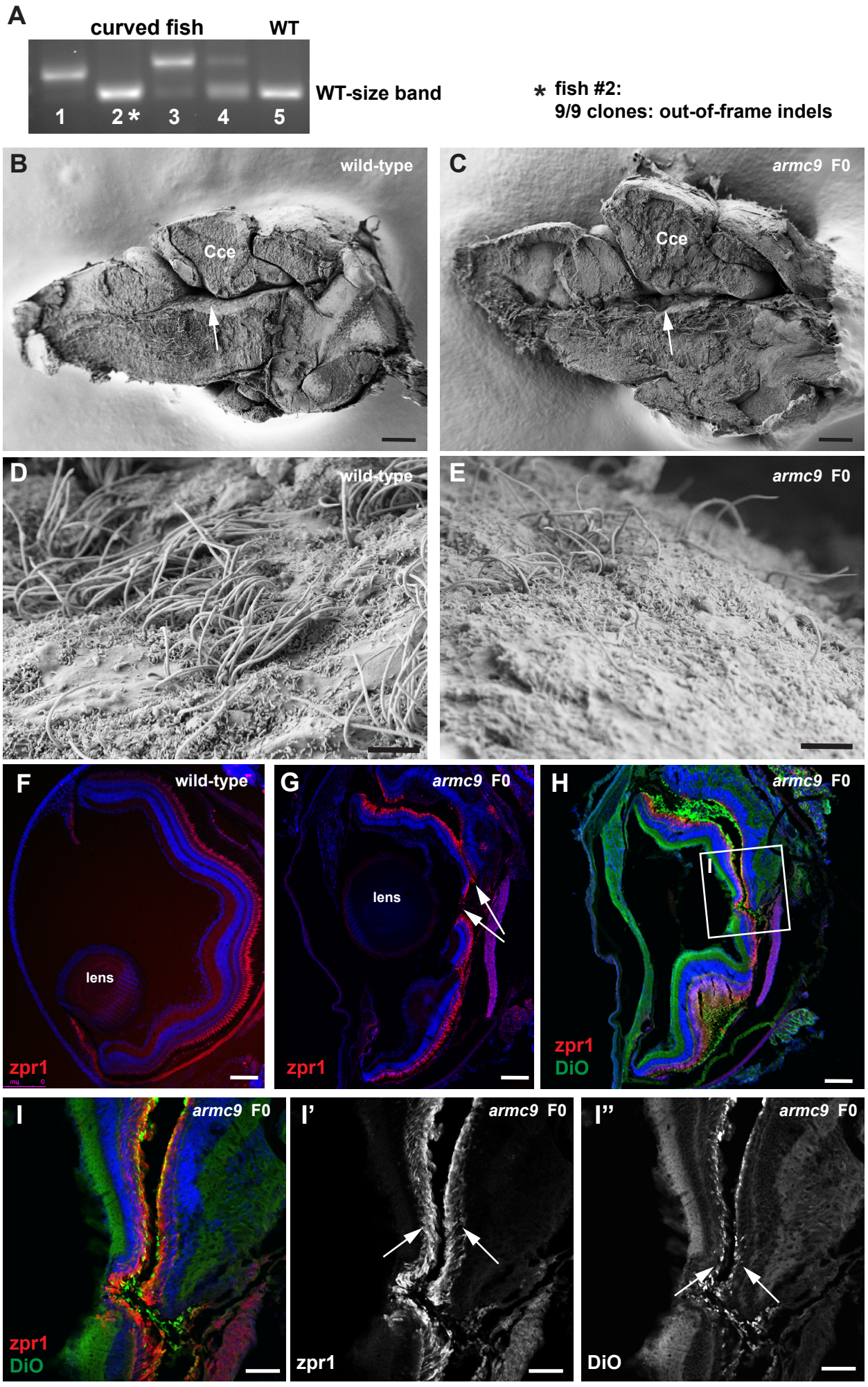
A
curved fish
WT
1
2*
3
4
5
WT-size band
* fish #2:
9/9 clones: out-of-frame indels
B
wild-type
Cce
C
armc9 F0
Cce
D
wild-type
E
armc9 F0
F
wild-type
lens
zpr1
G
armc9 F0
lens
zpr1
H
armc9 F0
I
zpr1
DiO
I
armc9 F0
zpr1
DiO
I'
armc9 F0
zpr1
I''
armc9 F0
DiO

Fig S3: ARMC9 antibody validation

(A) Western blot analysis of hTERT-RPE cells transfected with non-targeting control siRNA and siARMC9. Cell lysates were probed with antibodies to ARMC9 and GAPDH as loading control. **(B)** Quantification of western blot signal in (A) quantified via densitometry normalized to GAPDH.

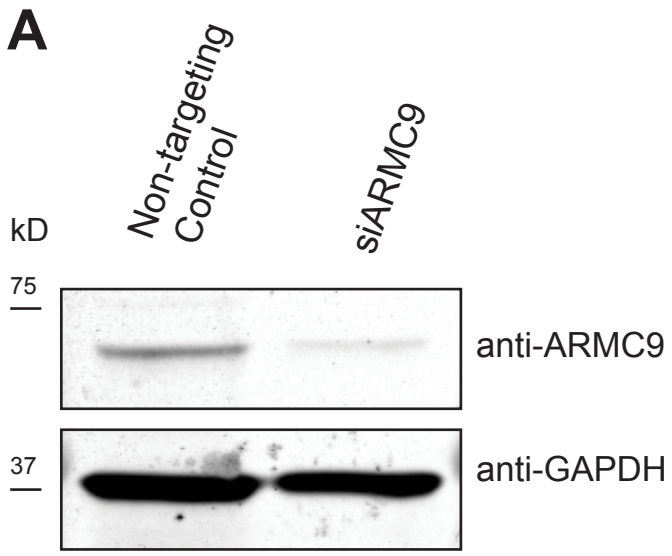
A
Non-targeting Control
siARMC9
kD
75
anti-ARMC9
37
anti-GAPDH

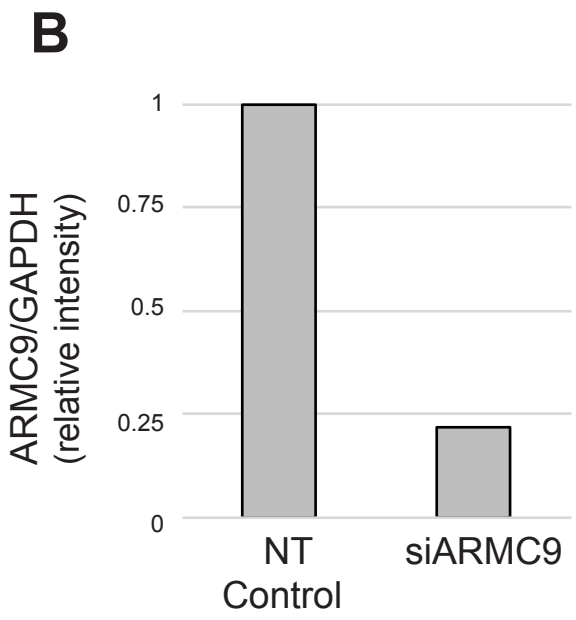
B
ARMC9/GAPDH (relative intensity)
1
0.75
0.5
0.25
0
NT Control
siARMC9

Table S1. Oligonucleotide primers for qPCR

Target Gene	**Primer ID**	**Sequence (5'-3')**
ARL13B Exons 2/3	Forward:	AATGCTGGTAAAACCGCAAC
	Reverse:	TTCCCCGAATTCTTATTCCA
ARMC9 Exons 21/22	Forward:	GGAGTGACCACCAGGGAATG
	Reverse:	GGCCACACGAAGAGAACAGA
ARMC9 Exons 3/4	Forward:	GAGACCGGACAAAGAGGAGC
	Reverse:	CTCTGTGGTCTGGCTCAAGG
ARMC9 Exons 2/3	Forward:	TTCCATCCGAGATGGGGACT
	Reverse:	GCTCCTCTTTGTCCGGTCTC
GAPDH Exons 2/6	Forward:	AGGTGAAGGTCGGAGTCAAC
		TTCACACCCATGACGAACAT

Table S2. Brain imaging findings in individuals with *ARMC9*-related Joubert syndrome

UW#	UW132-3	UW132-4	UW348-3	UW116-3	UW335-3	UW335-4	UW349-3	LR09-023	SA1-3	SA2-3	SA2-4
Age at MRI	29 yr	18 yr	10 mo	6 mo	2 mo	16 mo	7 mo	1 mo	14 mo	2 yr	4 yr
Molar Tooth Sign	Y	Y	Y	Y	Y	Y	Y	Y	Y	Y	Y
Agenesis of the corpus callosum	N	N	N	N	N	N	N	N	N	N	N
Ventriculomegaly	N	N	mild	mild	N	N	N	N	mild	N	N
PMG	N	N	N	N	N	N	N	N	N	N	N
Heterotopia	N	N	N	Y	N	Y	N	Y	N	N	N
Pituitary bright spot	P	P	P	P	P	P	A	P	A	P	P
Superior cb dysplasia	Y	Y	Y	Y	Y	Y	Y	Y	Y	Y	Y
cb hemisphere dysplasia	N	N	N	N	N	Y	N	Y	N	Y	N
cb atrophy	Y	Y	N	N	N	N	N	N	N	N	N
cervicomedulary heterotopia	N	N	unk	N	N	N	Y	possible	N	N	N
Foramen magnum cephalcele	unk	N	N	N	N	N	Y	possible	Y	N	N
		moderate-size retro-cb fluid		single L occipital PVNH		single L occipital PVNH	kinked brainstem	large posterior fossa with retro-cb fluid, single L temporal PVNH			thick corpus callosum

A=Absent, cb=cerebellar, L=Left, mo=months, N=No, P=Present, PMG=PolyMicroGyria, PVNH=PeriVentricular Nodular Heterotopia, unk=unknown, Y=Yes, yr=years,